IEEE WLANs in 5 vs 6 GHz: A Comparative Study

Hao Yin University of Washington Seattle, Washington, United States haoyin@uw.edu Sumit Roy University of Washington Seattle, Washington, United States sroy@uw.edu Sian Jin University of Washington Seattle, Washington, United States sianjin@uw.edu

ABSTRACT

US Federal Communications Commission (FCC) has adopted new rules to open the 6 GHz bands for unlicensed access as the increasing demand for wireless networks. The new ruling limits operation by a Power Spectral Density (PSD) limit in 6 GHz bands that differs from the total average power independent of the channel bandwidth in 5 GHz bands. The new power rules impact the transmission range, and the unequal power of the Access Points (AP) and stations (STA) also impact the system performance in wireless local area networks (WLANs). In this paper, we analyze the throughput of Wi-Fi distributed coordination function (DCF) with two physical (PHY) layer considerations, including the different power rules in 5 and 6 GHz bands as well as the unequal power setup among APs and STAs. To our best knowledge, this is the first work to analyze the cross-layer performance of Wi-Fi in 6 GHz bands and unequal power setups. Using ns-3 simulations, we validate our throughput analysis results and show the related insights.

CCS CONCEPTS

 Networks → Wireless local area networks; Wireless channel access; Network performance evaluation; • Network Simulation → ns-3.

KEYWORDS

Wi-Fi, 802.11, 6 GHz, ns-3, DCF, PHY, MAC, performance analysis, unequal power

ACM Reference Format:

Hao Yin, Sumit Roy, and Sian Jin. 2022. IEEE WLANs in 5 vs 6 GHz: A Comparative Study. In *Proceedings of the WNS3 2022 (WNS3 2022), June 22–23, 2022, Virtual Event, USA*. ACM, New York, NY, USA, 8 pages. https://doi.org/10.1145/3532577.3532580

1 INTRODUCTION

With demand for wireless broadband access continuing to escalate, there is increased pressure to allocate more spectrum for 5G and beyond services and for continuing efficient usage of the spectrum. Since IEEE 802.11 wireless local area networks (WLANs) carry an increasing proportion of wireless access traffic (\sim 60% of all 5G traffic will go over Wi-Fi networks by 2022), there is significant interest in expanding allocations for unlicensed spectrum, particularly in



This work is licensed under a Creative Commons Attribution International 4.0 License.

WNS3 2022, June 22–23, 2022, Virtual Event, USA © 2022 Copyright held by the owner/author(s). ACM ISBN 978-1-4503-9651-6/22/06. https://doi.org/10.1145/3532577.3532580

the mid-band $(1-6~{\rm GHz})$ region. As tracked by Cisco Annual Internet Report [3], the number of Wi-Fi hotspots is expected to grow four-fold and the average network connection speeds triple from 2018 to 2023.

This has led to new rulemaking by the US Federal Communications Commission (FCC) that opened the 6 GHz spectrum (5.925 to 7.125 GHz) ¹ [6] for unlicensed use. FCC has proposed two types of usage: indoor and outdoor. Indoor operations are allowed over the whole band using lower power devices; outdoor operations are possible under an Automated Frequency Coordination (AFC) regime to protect numerous licensed incumbents, including point-to-point microwave links, fixed satellite and TV broadcast services. As summarized in Table 1, the emission limits for indoor operation place the usual cap on total average per-user power independent of the channel bandwidth in conjunction with a Power Spectral Density (PSD) limit. The PSD limit for 6 GHz operation has been set at 5(-1) dBm/MHz for AP(STA), implying that for channel bandwidth less than 160 MHz, the average transmit power for AP or client devices is 3 dB lower than the corresponding 5 GHz scenario. The new rules have an impact on the transmission range for IEEE 802.11ax based devices that are designed to operate on variable channel bandwidth.

Further, client devices are power-limited operationally to preserve battery life, implying that the maximum transmit power of clients (STAs) is lower than the Access Points (AP). The transmit power impacts the desired link signal-to-noise ratio (SNR) as a function of the distance, and also any co-channel interference to neighboring basic service set (BSS) on the same channel. Hence the different transmit powers may potentially impact PHY performance and key parameters such as transmission range. Further, the new 802.11ax and 802.11be standards have incorporated several new MAC features like channel bonding and enhanced spatial reuse via BSS coloring; network-level analysis of such new features will also be impacted by the 6 GHz emission rules. Ours is one of the first studies to comparatively explore these aspects as a function of varying channel bandwidths. Our approach builds on the celebrated analytical model for Wi-Fi medium access control (MAC) [2] as a prelude to a simulation study conducted with the ns-3 simulator's current 802.11ax model implementation [5]. Wi-Fi channel access in a single cell based on Carrier-Sense Multiple Access with Collision Avoidance (CSMA/CA) was modeled by [2] for predictions of throughput. The model expresses the node back-off process with a two-dimensional Markov chain (hereinafter, Markov Chain model) assuming identical node transmit power and ideal physical layer (no errors) and under saturation (nodes always have data to send and hence are always in contention) conditions. Thereafter, several extensions have followed, such as [11] where the authors considered

 $^{^1\}mathrm{The}$ attenuation is higher in the 6 GHz band than in the 5 GHz bands, but it's less significant compared with the changing of the power rules.

Table 1: (Max) Average Transmit Power vs. Channel Bandwidth: Indoor Operation by FCC

Device type	Frequency	Max power for bandwidth			
		20 MHz	40 MHz	80 MHz	160 MHz
Low power AP	6 GHz	18.01 dBm	21.02 dBm	24.03 dBm	27.04 dBm
	5 GHz	30 dBm	30 dBm	30 dBm	30 dBm
Low power STA	6 GHz	12.04 dBm	15.05 dBm	18.06 dBm	21.07 dBm
	5 GHz	24 dBm	24 dBm	24 dBm	24 dBm

more realistic back-off slots probabilities, [9] that incorporated non-saturation conditions, and [4] that extended it to include non-ideal channel and capture effects. However, the impact of the unequal transmit powers between AP and stations on performance is rarely discussed.

The primary purpose of this study is to investigate the impact of the new FCC 6 GHz emission rules on Wi-Fi network throughput and coverage, in cognizance of unequal transmit powers. To achieve this, we propose new extensions to the Markov Chain model in cognizance of modeling the cross-layer (PHY and MAC) features needed for performance prediction. The major contributions of this paper are as follows:

- Enhance the well-known Markov chain model by incorporating PHY frame error rate for an Additive White Gaussian
 Noise (AWGN) channel and comparing the resulting throughput to simulation results from the ns-3 network simulator.
- Improve the system model by considering unequal powers among AP and STAs to explore the impact on network throughput.
- Conduct comparative analysis for throughput under the different FCC emission rules for 5 GHz and 6 GHz.

The remainder of this paper is organized as follows. The outline of the Markov chain model and the theory of the parameters considered are described in Section 2, then we show the effects of these parameters and propose a throughput analysis method. The simulation results are shown in Section 4. Section 5 concludes this paper.

2 SYSTEM MODEL

2.1 Setup

We consider a single cell network shown in Figure 1. For initial convenience, all stations are distributed on the same distances *d* meters from the AP. All nodes are assumed with single-input single-output (SISO) PHY - i.e., a single transmit and receive antenna, respectively. All fixed length PHY packets are sent using a common transmit power P_{TX} over a channel bandwidth B. The transmitted packets are passed through a frequency-flat wide-band channel with free space path loss and additive Gaussian noise at the receiver. Each receiver attempts to decode the received packet with corresponding receiver (RX) SNR; the receive chain performance is mapped into a packet error rate (PER) P_e using an AWGN-SISO PER-SNR lookup table for the corresponding modulation and coding scheme (MCS), as already implemented [8, 10]. The PER P_e is then used to obtain the single-cell throughput. This methodology can be readily extended to other complex channel models (non-AWGN-SISO) based on the corresponding PER-SNR mappings.

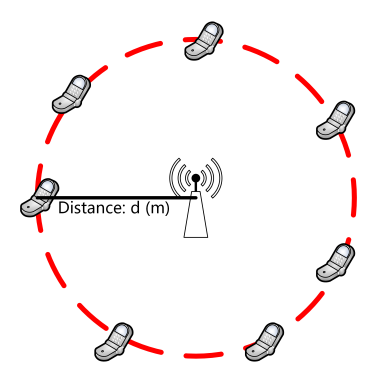


Figure 1: System Setup

2.1.1 RX Chain Processing. Noise figure (N_{figure}) and noise factor (F) are measures of degradation of the SNR caused by the design and implementation of various components in the RX signal chain. The noise factor is the ratio of the output noise power of any system component relative to (baseline) thermal noise power at the device input (usually measured at a reference temperature $T_0 = 290 \text{ K})^2$. The noise figure N_{figure} is the noise factor in dB: $N_{figure} = 10 \log_{10}(F)$, where $F = 1 + \frac{T_e}{T_0}$, T_e is the device's noise temperature.

The power spectral power density of thermal white noise is the noise power in a bandwidth of 1 Hz, i.e., $N_0 = kT(W/Hz)$, where k is Boltzmann's constant that equals $1.3803 \times 10 - 23$ J/K (or W/(K.Hz)), and T is the temperature in degrees kelvin³. Using this, it follows that the minimum equivalent input noise for a receiver at room temperature (290 K) is -174 dBm/Hz. Hence the thermal noise $N_{thermal}$ power in a bandwidth of B Hertz is $N_{thermal} = kTB$, and the total noise power in B Hz (in dBm) is thus

$$\begin{split} N_{floor} &= N_{figure} + 10 \log_{10}(N_{thermal}) \\ &= -174 + N_{figure} + 10 \log_{10}(B). \end{split} \tag{1}$$

2.1.2 Link Budget. A link budget accounts for all gains and losses in a communication chain that the transmitted signal experiences from a transmitter (TX), through a medium to the receiver. It provides a relation for the received signal power (S_{RX}) at the receiver input corresponding to the transmitter signal power (S_{TX}) emitted as follows:

$$S_{RX} = S_{TX} + G_{TX} + G_{RX} - L_{PL},$$
 (2)

where L_{PL} is the path loss and the antenna gains (G_{TX} and G_{RX}) includes any feedline and other losses. For free-space propagation: the distance and frequency dependant propagation loss is given by

$$L_{PL} = 20\log(d) + 20\log(f) + 20\log(d) + 20\log(\frac{4\pi}{c}),$$
 (3)

where d is the TX-RX distance, f is the center frequency of the transmitted signal, and c is the speed of light.

 $^{^2}$ The noise factor is thus the ratio of input SNR to output SNR of any device component, representing its contribution to overall noise power.

³Note Watt = $J/\sec = J \cdot Hz$

2.1.3 RX SNR and PER. The RX SNR over a frequency-flat AWGN-SISO channel is defined as

$$\gamma_{RX} = \frac{S_{RX}}{N_{floor}},\tag{4}$$

where N_{floor} is given in Eq. (1) and P_{RX} is given in Eq. (2). For obtaining PER from RX SNR, ns-3 stores the PER-SNR lookup tables⁴ over the frequency-flat AWGN-SISO channel and a reference packet length l_0 under different MCSs. For estimating PER P_e for any desired packet length l, ns-3 conducts the following two steps: (1) The RX SNR γ_{RX} is first mapped into the PER $P_{e,0}$ at the reference packet length $l_0=1458$ Bytes using the stored PER-SNR lookup table under the simulated MCS. (2) Next, PER interpolation formula [7] is used to obtain the PER under the simulated packet length l:

$$P_e = 1 - (1 - P_{e,0})^{l/l_0}. (5)$$

Note that above PER P_e generally applies to both AP and STA with any suitable modification to account for differences in transmit power P_{TX} ; we denote the corresponding PER at the AP and STA using the superscript 'AP' and 'STA'. Since the transmit power of the AP P_{TX}^{AP} is larger than the transmit power of STAs P_{TX}^{STA} , the PER P_e^{el} for uplink transmission is lower than the PER P_e^{el} for the downlink. In the following throughput analysis, we will investigate the impact of unequal powers between AP and STAs.

2.2 Throughput Analysis: Imperfect PHY

An accurate analytical model for IEEE 802.11 WLAN operation based on Distributed Coordination Function (DCF) for a single network with saturated nodes, was originally presented in the reputed work [2]. The 2-D Markov model in the original was refined in [4] considering the non-ideal transmission channel. In saturation conditions, every station always has a frame available for transmission after the completion of each successful transmission and must wait for a random backoff duration before channel access. The backoff is performed in discrete time units called slots, and all stations are assumed synchronized on the slot boundaries. The maximum value of the current backoff counter for each station also depends on its transmission history (e.g., how many retransmissions the head-of-line frame has suffered). The process representing the backoff counter evolution, in general, is non-Markovian, but on the assumption that at each transmission attempt, the frame collision probability is constant and independent of all other nodes, the Markov chain model developed by [2] and reproduced in Figure 2 provides accurate predictions.

Using this Markov model, the probability that a station transmits in a randomly chosen slot time at the channel contention period is given by Eq. (6):

$$\tau = \frac{2}{W_0 \left(\frac{(1 - (2P)^{m+1})(1 - P) + 2^m (P^{m+1} - P^{R+1})(1 - 2P)}{(1 - 2P)(1 - P^{R+1})} \right) + 1}$$
 (6)

where *R* is the number of the backoff stage (R = m + 1 in Figure 1), W_0 is the minimum contention window size - 1, $m = \log_2(\frac{CW_{max}}{CW_{min}})$

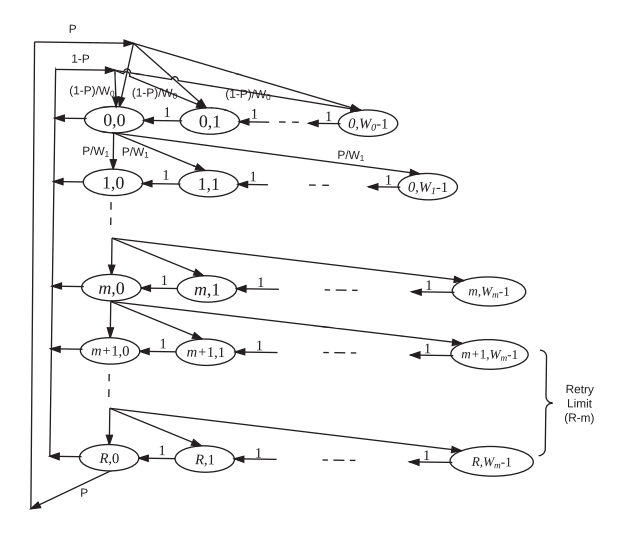


Figure 2: Markov Model for DCF

and *P* is the probability of failed transmission, given by Eq. (7):

$$P = 1 - (1 - P_e)(1 - P_c) = P_e + P_c - P_e P_c.$$
 (7)

Note that now, *two* factors cause changes to the backoff window due to a failed transmission. Failure due to MAC collisions occurs with probability P_c on the transmitted packets, while PHY transmission errors due to the channel occur with probability P_e . We assume that collisions and transmission error events are statistically independent. The constant MAC collision probability is given by Eq. (8):

$$P_c = 1 - (1 - \tau)^{n-1} \tag{8}$$

where n is the number of competing stations.

The three equations (6), (7), and (8) with three variables can be solved to obtain τ , P and P_c for a give PHY frame error rate P_e . At each idle slot, nodes are competing for the channel access, and only when the backoff window count drops to 0, the node get channel access for the current slot. So the probability of at least one node transmitting in a slot is given by Eq. (9):

$$P_{tr} = 1 - (1 - \tau)^n. (9)$$

If two or more nodes have the backoff window count of 0 at the same slot, the collision happens. Thus the successful transmission happens if and only if one node has 0 countdown, and the successful transmission probability P_s is then calculated as in Eq. (10):

$$P_s = \binom{n}{1} \frac{\tau (1 - \tau)^{n-1}}{P_{tr}} = \frac{n\tau (1 - \tau)^{n-1}}{P_{tr}}.$$
 (10)

Using obtained P_{tr} and P_s , the normalized throughput Tpt can be calculated according to Eq. (11):

$$Tpt = \frac{P_{s}P_{tr}E[Pkt]}{(1 - P_{tr})\sigma + P_{tr}P_{s}(1 - P_{e})T_{s} + P_{tr}(1 - P_{s})T_{c} + P_{tr}P_{s}P_{e}T_{e}},$$
(11)

where T_s is the average time that the channel is sensed busy due to successful transmission, T_c due to collision and $T_e = T_c$ due to the

 $^{^4}$ One example table for HeMcs5 is summarised in table 3.

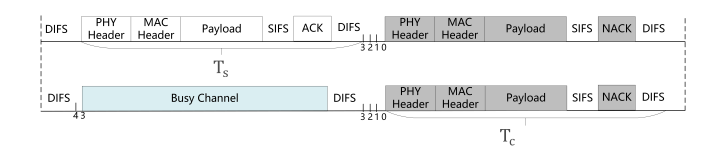


Figure 3: Graphic Illustration of Successful Transmission and Collision with DCF Basic Mechanism

channel error. As illustrated in Figure 3, the transmission time can be calculated in Eq. (12) and (13):

$$T_s = H + E[Pkt] + SIFS + \delta + ACK + DIFS + \delta, \tag{12}$$

$$T_c = H + E[Pkt] + \delta + EIFS, \tag{13}$$

where E[Pkt] is the mean frame duration of the packets. Here Hrepresents the MAC and PHY header time, and δ is the propagation delay equal to 0.1 μ s. SIFS, DIFS and EIFS = SIFS + NACK + DIFS are time duration specified in 802.11 standard required for a wireless interface to process a received frame and to respond with a response frame.

The data rate for different MCS is calculated in Eq. (14):

$$DataRate = \frac{N_{SD,U} * N_{BPSCS,U} * r_c}{T_{DFT} + T_{GI}}, \tag{14}$$

where $N_{SD,U}$ is the number of data subcarriers per resource unit, $N_{BPSCS,U}$ is the number of coded bits per subcarrier per stream for the resource unit, and r_c is coding rate. T_{DFT} and T_{GI} are the OFDM symbol duration and guard interval duration. The value of those parameters are defined in different IEEE standards for different modulation scheme.

THROUGHPUT ANALYSIS: UNEQUAL 3 TRANSMIT POWER

Among the Wi-Fi devices, STAs are typically power-limited and their maximum transmit power is lower than that of APs, for energy conservation to prolong battery life. The lower transmit power reduces the SNR for the uplink compared with the downlink for the same link distance, leading to potentially different P_e . So we extend the analytical model to capture the impact of the unequal power by incorporating different P_e for the uplink and downlink traffic, by introducing P_e^{ul} and P_e^{dl} for the transmission failure probability P^{STA} and P^{AP} respectively. From CSMA/CA MAC perspective - a link loss due to P_e is treated the same as a collision and leads to an increase of the backoff window, so this also impacts 'effective' collision probability P_c , and the access probability τ . Hence the collision probability in Eq. (8) now can be written for AP and STAs, respectively:

$$P_c^{AP} = 1 - (1 - \tau^{STA})^{n-1},\tag{15}$$

$$P_c^{AP} = 1 - (1 - \tau^{STA})^{n-1},$$

$$P_c^{STA} = 1 - (1 - \tau^{AP})(1 - \tau^{STA})^{n-2}.$$
(15)

We can substitute P_c back to Eq. (6) and (7) to get τ^{STA} , and τ^{AP} , leading to a set of six equations and six variables, which needs to be solved numerically. A simple and effective process adopted follows by using an interactive approach: since all the variables are probabilities, we sample values from (0, 1) for some input variables and calculate the rest (output) using the equations sequentially. For instance, we sample 1000 points uniformly from (0,1) for P_c^{STA} , Algorithm 1: Interactive Algorithm to Obtain the Probability Variables

- 1. Sample values from (0, 1) for P_c^{STA} uniformly, i.e.
- $P_c^{STA} = range(0.0, 1.0, 1000);$ 2. Calculate $P^{STA} = P_c^{STA} + P_e^{STA} P_c^{STA} P_e^{STA};$ 3. Calculate the τ^{STA} using Eq. (6) (τ^{STA} only depends on
- 4. Calculate P_c^{AP} using Eq. (15) and then calculate P^{AP} , τ^{AP} sequentially similar as step 2, 3;
- 5. Obtain \hat{P}_c^{STA} from τ^{AP} and τ^{STA} using Eq. (16);
- 6. Find the i^{th} sample that has the minimum error:

$$\widetilde{j} = \arg\min | \hat{P}_c^{STA} - P_c^{STA} |$$

7. Finally, get all the variables as the \tilde{j}^{th} value in the vectors.

and then calculate the τ^{STA} by Eq. (7) and (6) for all points. With τ^{STA} , we can then calculate P_c^{AP} from Eq. (15) and get τ^{AP} and P^{AP} . We finally obtain \hat{P}_c^{STA} using the results of τ^{AP} and τ^{STA} and compare the input P_c^{STA} with \hat{P}_c^{STA} and select the P_c^{STA} that yields the minimum error. This interactive algorithm to obtain the variables is summarized in Algorithm 1.

Now we consider the calculation of *Tpt*. For the AP and STAs, the transmission time T_s and the collision time T_c remain the same, and we can consider the normalized throughput as two parts, the throughput during the whole time frame for AP Tpt^{AP} and stations Tpt^{STA} respectively, i.e., $Tpt = Tpt^{AP} + Tpt^{STA}$. Then according to Eq. (11), we need to re-calculate the P_{tr} and P_s for stations and AP. The probability P_{tr}^{STA} or P_{tr}^{AP} of at least one station or AP (node) transmitting in a slot are now:

$$P_{tr}^{AP} = P_{tr}^{STA} = 1 - (1 - \tau^{AP})(1 - \tau^{STA})^{n-1},\tag{17}$$

For the probability P_s^{STA} or P_s^{AP} of successful transmission are

$$P_s^{STA} = \frac{(n-1)\tau^{STA}(1-\tau^{AP})(1-\tau^{STA})^{n-2}}{P_{tr}^{STA}},$$
 (18)

$$P_s^{AP} = \frac{\tau^{AP} (1 - \tau^{STA})^{n-1}}{P_{tr}^{AP}}.$$
 (19)

NS-3 SIMULATION & VALIDATION

In this section, we present results using the ns-3 802.11ax model [5] and compare with the predictions from analytical model in Section 2 ⁵. The simulation setup is shown in Fig 1 for a single cell, where stations are uniformly distributed on a circle at a distance of d meters. Nodes in 802.11ax network transmit with parameters summarized in Table 2. All nodes use the same HeMCS5 and corresponding DataRate = {68.8, 137.6, 288.2, 576.5} Mbps for {20, 40, 80, 160} MHz channel respectively, per Eq. (14) with parameters in [1]. We consider two scenarios: 1) Uplink only to investigate the impact on transmission range of the different power rules for 5 GHz and 6 GHz bands. 2) Both Uplink & Downlink based on the different transmit power for AP and STAs to explore the impact of the unequal power.

 $^{^5}$ The simulation code is available: https://github.com/Mauriyin/ns3/tree/unequal

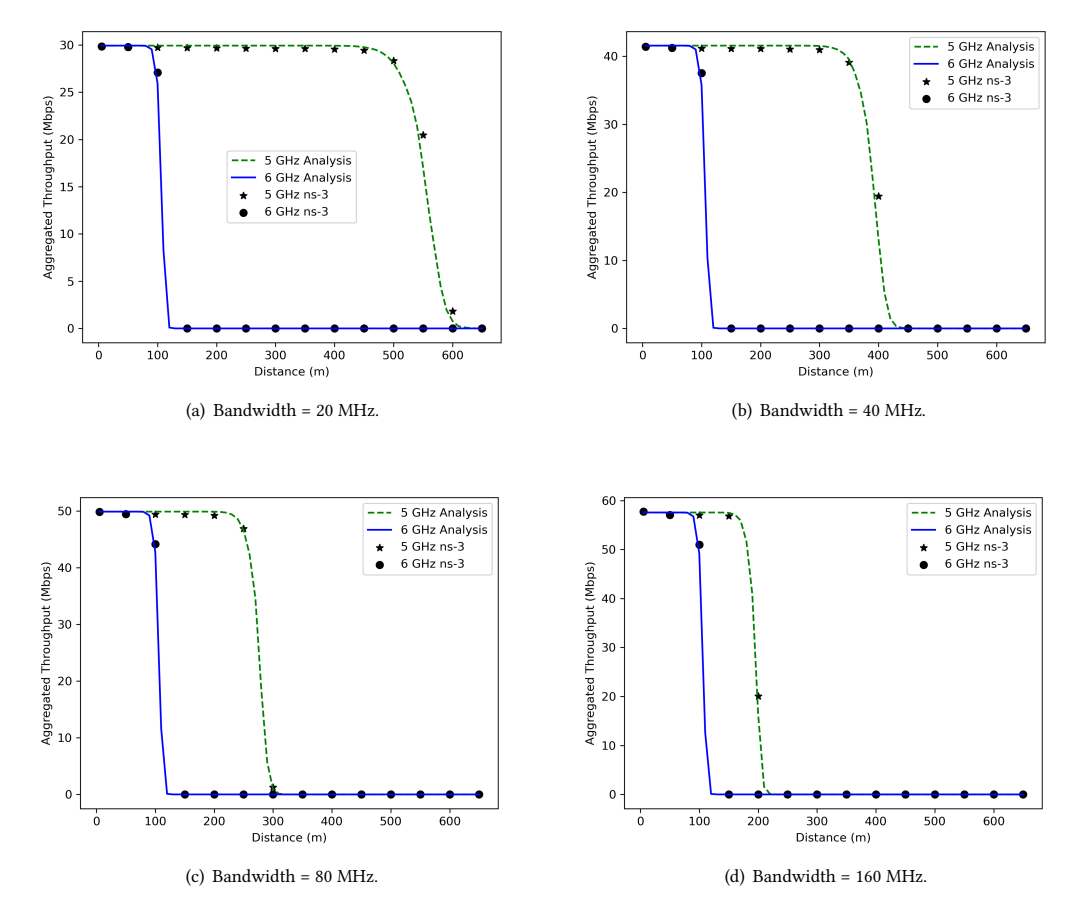


Figure 4: Simulation Results of Different Bandwidth for Uplink Only Case. Total 5 Stations and HeMcs = 5. Using the Maximum Power Defined in Table 1

Table 2: Parameters for Simulation (802.11ax)

Slot time σ (μ s)	9		
SIFS (μs)	16		
DIFS (μs)	34		
EIFS (μs)	SIFS + ACK + DIFS		
PHY preamble & header duration(μ s)	20		
Upper Layer Headers (Bytes)	36		
OFDM Guard Interval (μs)	0.8		
CW_{min}	16		
CW_{max}	1024		
m	6		
Aggregation Type	None		
Propagation model	LogDistancePropagationLossModel		
Error model	TableBasedErrorRateModel		

4.1 Uplink Only

In this scenario, five stations send packets to the AP in saturation mode with the same maximum power according to the FCC 5 GHz and 6 GHz power limits in Table 1 6 . In Figure 4, the solid line

represents the analytical model predictions in Section 2, close to the obtained ns-3 simulation results. When the distance is very close from the stations to the APs, there is no PHY error that happens. The normalized throughput calculated from Eq. (6) - (11) is 0.431 for 20 MHz channel. The aggregated throughput then equals $DataRate \times Tpt = 68.8 \times 0.431 = 29.7$ Mbps for HeMCS5. As the bandwidth increases, the normalized throughputs are 0.301, 0.173, and 0.100 for 40 MHz, 80 MHz, and 160 MHz channels, respectively. Note that as the channel bandwidth increases, for fixed packet length, the duration of the data packet E[Pkt] drops while overheads like legacy PHY header, DIFS, and SIFS remain the same. Hence throughput does not increase in proportion to the channel bandwidth, suggesting the utility of MAC frame aggregation to increase Layer-2 efficiency.

As the distance increases, the received power P_{RX} and SNR decreases, the packet error rate increases, and the aggregated throughput drops. The average transmit power of 5 GHz is higher than the 6 GHz band, so the transmission range without PHY error of the 5 GHz band is larger. As the channel bandwidth increases, the transmission range of the 5 GHz band decreases while the transmission range in the 6 GHz band remains the same. While the average transmit power for the 5 GHz band remains the same with varying

 $^{^6}$ Note the setups are simplified so it may not be realistic in real world, i.e., the transmission range can't reach as far as 600 m.

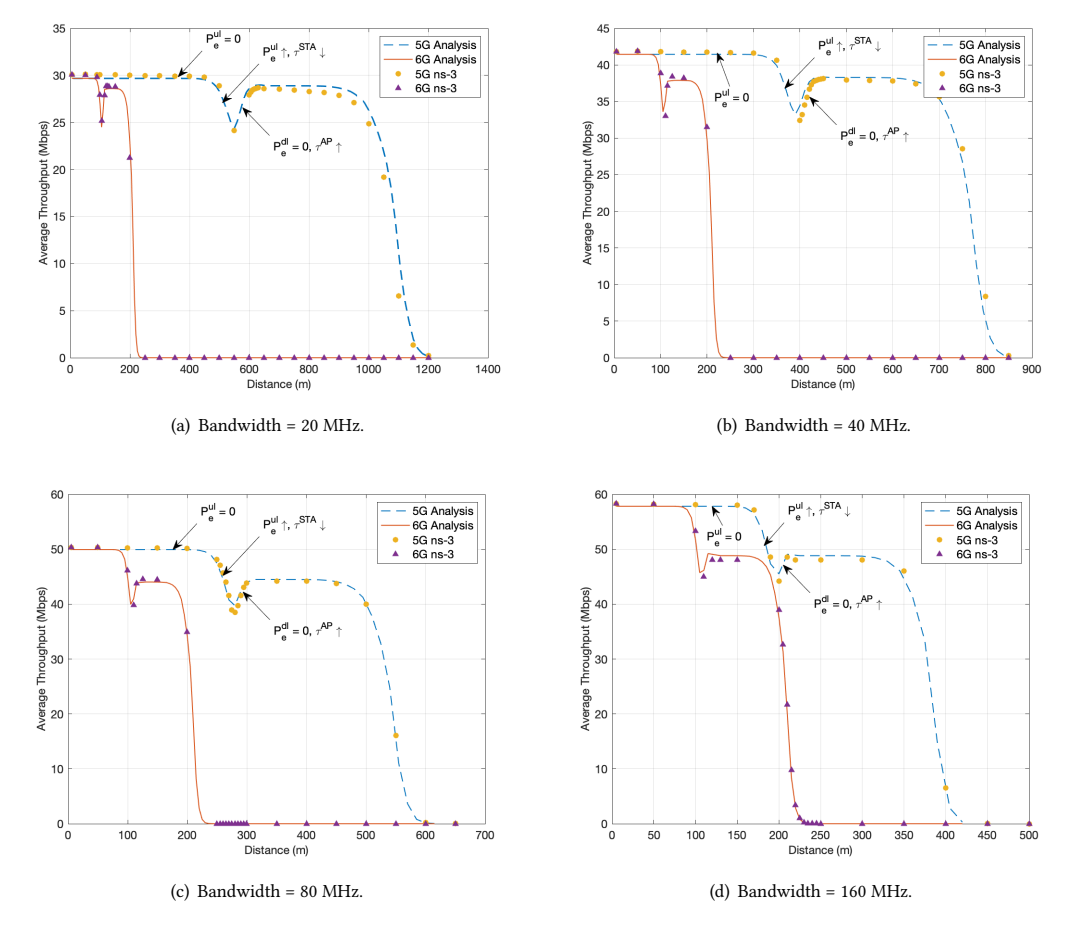


Figure 5: Simulation Results of Different Bandwidth for Unequal Power Case and HeMcs = 5. Using the Maximum Power Defined in Table 1

bandwidths, the noise power increases with the channel bandwidth, hence the SNR decreases. However, for the 6 GHz band, the SNR remains the same since both signal and noise power are now proportional to bandwidth. Note that the peak aggregate throughput increases in both cases with bandwidth, as expected.

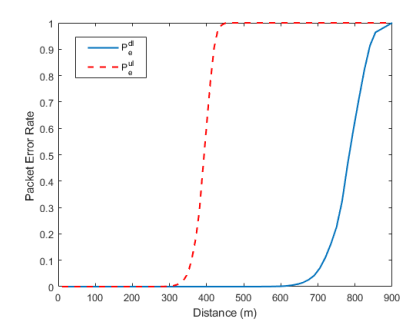
In general, the transmit power of 6 GHz devices is lower than 5 GHz, implying lower coverage. Since Wi-Fi devices have the capability to operate on multiple bands - notably via the *multi-link* operation feature in 802.11be that allows simultaneous transmission on two 20 MHz channels, e.g., one each from 5 and 6 GHz, respectively - such asymmetry in coverage will limit desired performance improvements

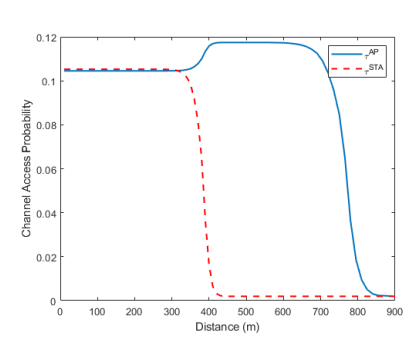
4.2 Uplink & Downlink with Unequal Power

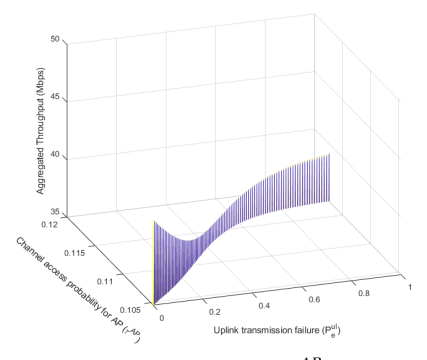
In Wi-Fi networks, the transmit power of client devices is normally lower than the AP, per the power limits suggested by FCC to conserve battery life. To investigate the impact of the unequal power, we conduct simulations according to the maximum power limit in Table 1. One AP and four stations are competing for channel access where all nodes are in saturation mode. Anytime AP gains channel

access, it sends packets to one of the stations randomly at each time slot.

The simulation results are shown in Figure 5. In general, changing the transmission range and the bandwidth has the same impact as the uplink only case. However, unlike the smooth drop in Figure 4 as the distance increases, there is a noticeable 'undershoot' in throughput in the unequal power case. As the network distance increases and SNR drops, some PHY layer errors occur. For example, in the 5 GHz case of Figure 5(b), between 300 m to 390 m, the throughput drops, as shown in Figure 4(b) and thereafter between 390 m to 420 m, the throughput recovers. The reason for such an undershoot in throughput is explained in Figure 6. At distances 300 m to 420 m, the SNR for downlink is still sufficient for decoding of the MCS, so no PHY errors occur for AP downlink transmission, but some errors occur for the stations uplink, as shown in Figure 6(a). This leads to two effects. On the one hand, the packet errors for station uplink (P_e^{ul}) decrease the aggregate throughput. On the other hand, the backoff window for the STA increases in response to PHY errors and the AP gets more chance to access the







(a) Packet error rate for AP P_e^{dl} and for STA P_e^{ul} as the (b) Channel access probability for AP τ^{AP} and for STA (c) Channel access probability for AP τ^{AP} and throughput distance changes. τ^{STA} as the distance changes. changing as the P_e^{ul} changes.

Figure 6: Channel Access Probability τ and Throughput Changing as the P_e^{ul} Changes. HeMcs=5, Bandwidth=40 MHz, Frequency=5 GHz. $P_{TX}^{STA}=24$ dBm and $P_{TX}^{AP}=30$ dBm

channel $(\tau^{AP} \text{ increases})^7$, as shown in Figure 6(b). This increases the throughput. We show the combination of the two effects in Figure 6(c), which shows the aggregate throughput as a function of τ^{AP} and P_e^{ul} .

The results in Figure 5 can also be analyzed using the equations (11) - (13). As $P_e^{ul} \rightarrow 1$ outside transmission range, transmissions fail all the time for stations; therefore the contention window of the stations will always keep the largest value, i.e., $W_0 = CW_{max} - 1 = 1023$ and m = 0. We then calculate the probability τ^{STA} that the stations transmit at each slot by substituting in Eq. (6), i.e., $\tau^{STA} = \frac{2}{1024}$. The transmission of AP may also collide with stations in saturation mode. The collision probability for the AP now can be calculated from $P_c^{AP} = 1 - (1 - \tau^{STA})^{n-1}$, and thereafter P_w and τ^{AP} using Eq. (6) and (7). After obtaining the different transmission probability τ^{AP} and τ^{STA} , we also update the probability P_t that at least one node transmits in a slot and the probability P_s of successful transmission according to equations

$$P_{tr} = 1 - (1 - \tau^{STA})^{n-1} (1 - \tau^{AP}) \tag{20}$$

$$P_{s} = \frac{\tau^{AP} (1 - \tau^{STA})^{(n-1)}}{P_{tr}}.$$
 (21)

As shown in Figure 5, using the same backoff window and MCS for various devices may cause the drop of the system performance, especially in the dense and overlapping networks. What's more, the various transmit powers for uplink and downlink contribute to different interference levels. If the devices are aware of the traffic in overlapping networks, they can better adjust spatial reuse parameters like clear channel assessment energy detection (CCA-ED) threshold and overlapping BSS packet detection (OBSS-PD) threshold. Since the new 11be standard allows overlapping APs to coordinate with each other, the corresponding thresholds may be chosen within an enhanced cross-layer optimization that incorporates the unequal transmit powers.

4.2.1 Ring Deployment. Previous sections show the case where stations are uniformly distributed on a circle. Now, we consider three more general cases.

- Case 1: the stations are uniformly distributed within a ring bounded by the outer radius *d*1 and the inner radius *d*2, as shown in Figure 7(a);
- Case 2: the stations are uniformly distributed within a circle with radius d1;
- Case 3: the stations are uniformly distributed within a circle with three rings with radius d1, d2 = 0.7d1, and d3 = 0.3d1, as shown in Figure 7(b).

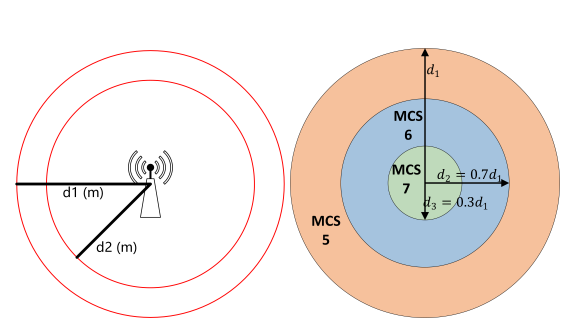
In cases 1 and 2, all the stations adopt the same MCS 5. In case 3, different stations in different rings adopt different MCSs, where the inner ring adopt MCS 7, intermediate ring adopt MCS 6 and outer ring adopt MCS 5, such that $P_e^{dl} \leq 0.1$ for MCS 6 and MCS 7 when $d1 \leq 200$ m. In these cases, the uplink PERs for different stations vary based on their ring location, so the prior equations do not apply. However, we conduct simulations using the ns-3 to verify whether the 'undershoot' still occurs. In the simulations, we treat d1 as a variable to explore the impact of broader AP coverage and consequent 'ring' widths on aggregate throughput.

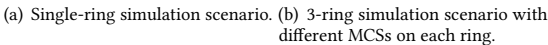
As shown in Figure 7(c), as the d1 increases, we still see the 'undershoot' for different $\frac{d2}{d1}$ values (Case 1). However, the minimum throughput value (at the bottom of 'undershoot') increases as $\frac{d2}{d1}$ decreases, i.e., the area of the ring is larger. In case 1, nodes have different PERs within a ring, so the distance of the minimum value increases. When the ring area is larger, more nodes are close to the AP, so the throughput is higher than the smaller ring area. In cases 2 and 3, we can still observe the 'undershoot', but the depth (minimum value) is much smaller. Further, in case 3, the aggregated throughput is higher relative to case 2 because of higher MCS for the stations in the innermost ring, closest to the AP.

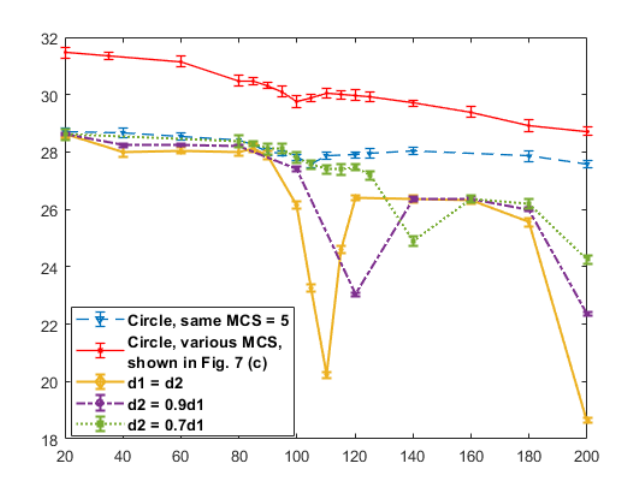
5 CONCLUSION

In this paper, we presented a cross-layer performance analysis model for the 802.11 WLANs based on different power rules and unequal power setup for uplink and downlink. The proposed model

 $^{^7}$ The au^{AP} represents the probability of the node accessing the channel in each idle slot. For our setup, the $CW_{min}=16$, so the maximum $au=\frac{1}{8}=0.125$, which can be obtained by substituting $W_0=15$, P=0 (no collision) and R=1 (always using the minimum backoff window setup) in Eq. (6).







(c) Simulation results for different d2 as d1 increases.

Figure 7: Simulation Results for Uniformly Distributed Stations within a Ring. Bandwidth=20 MHz, Frequency=6 GHz. P_{TX}^{STA} = $18.01 \text{ dBm and } P_{TX}^{AP} = 21.02 \text{ dBm}$

can now predict the aggregated throughput under various power rules and setups. Simulation results conducting by ns-3 show that the proposed model is accurate in the saturation test cases. This study shows the impact of power rules and setups on the transmission range, which are fundamental for designing and optimizing the spatial reuse features in 802.11 ax and 802.11 be. The observations from the unequal power setups also show that we need to consider the power difference for AP and devices so that we have more gains from the scheduling and spatial reuse decisions. In the future, we will extend the analytical model with a more realistic channel model and multi-bss setup to investigate the gains we can get for the dense overlapping networks in 5 GHz and 6 GHz bands.

ACKNOWLEDGMENTS

This work was supported in part by NSF CCRI ENS Award # 2016379.

REFERENCES

- [1] 2018. IEEE Draft Standard for Information Technology Telecommunications and Information Exchange Between Systems Local and Metropolitan Area Networks - Specific Requirements Part 11: Wireless LAN Medium Access Control (MAC) and Physical Layer (PHY) Specifications Amendment Enhancements for High Efficiency WLAN. IEEE P802.11ax/D3.0, June 2018 (2018), 1-682.
- [2] Giuseppe Bianchi. Mar. 2000. Performance Analysis of the IEEE 802.11 Distributed Coordination Function. IEEE Journal on Selected Areas in Communications 18, 3 (Mar. 2000), 535-547.
- [3] Cisco. Cisco System Inc., Mar. 2020. Cisco Annual Internet Report (2018–2023). White Paper (Cisco System Inc., Mar. 2020).
- [4] Fred Daneshgaran, Massimiliano Laddomada, Fabio Mesiti, and Marina Mondin. 2008. Unsaturated Throughput Analysis of IEEE 802.11 in Presence of Non Ideal Transmission Channel and Capture Effects. IEEE Transactions on Wireless Communications 7, 4 (2008), 1276-1286. https://doi.org/10.1109/TWC.2008.060859
- Sébastien Deronne, Thomas R. Henderson, Scott Carpenter, Leonardo Lanante, Sumit Rov, Morteza Mehrnoush, Malcolm Smith, and Poova Monajemi, 2019, ns-3 Wi-Fi 11ax project. https://depts.washington.edu/funlab/wp-content/uploads/ 2018/11/11ax-final-report.pdf

- [6] Federal Communications Commission. 2020. Report and Order and Further Notice of Proposed Rulemaking in the Matter of Unlicensed Use of 6 GHz Band. https://docs.fcc.gov/public/attachments/FCC-20-51A1.pdf IEEE TGax Group. 2016. IEEE P802.11 Wireless LANs: 11ax Evaluation Method-
- ology. (2016).
- Sian Jin, Sumit Roy, Weihua Jiang, and Thomas R. Henderson. 2020. Efficient Abstractions for Implementing TGn Channel and OFDM-MIMO Links in ns-3 (WNS3 2020). Association for Computing Machinery, New York, NY, USA, 33-40. https://doi.org/10.1145/3389400.3389403
- David Malone, Ken Duffy, and Doug Leith. 2007. Modeling the 802.11 Distributed Coordination Function in Nonsaturated Heterogeneous Conditions. IEEE/ACM Transactions on Networking 15, 1 (2007), 159-172. https://doi.org/10.1109/TNET. 2006.890136
- [10] Rohan Patidar, Sumit Roy, Thomas R. Henderson, and Amrutha Chandramohan. 2017. Link-to-System Mapping for ns-3 Wi-Fi OFDM Error Models. In Proceedings of the Workshop on ns-3 (Porto, Portugal) (WNS3 2017). Association for Computing Machinery, New York, NY, USA, 31-38. https://doi.org/10.1145/3067665.3067671
- [11] Ilenia Tinnirello, Giuseppe Bianchi, and Yang Xiao. 2009. Refinements on IEEE 802.11 Distributed Coordination Function Modeling Approaches. IEEE Transactions on Vehicular Technology 59, 3 (2009), 1055-1067.

A APPENDIX 1

A.1 PER-SNR lookup table

Table 3: PER-SNR Lookup Table for HeMcs5

SNR (dBm)	PER	SNR (dBm)	PER	SNR (dBm)	PER
20.0000	0.0000	18.3000	0.0042	16.5000	0.3154
19.8000	0.0000	18.0000	0.0081	16.3000	0.4842
19.5000	0.0001	17.8000	0.0159	16.0000	0.6689
19.3000	0.0002	17.5000	0.0302	15.8000	0.8463
19.0000	0.0005	17.3000	0.0589	15.5000	0.9474
18.8000	0.0008	17.0000	0.1054	15.3000	0.9871
18.5000	0.0020	16.8000	0.1791	15.0000	1.0000